Localization of Human TACC3 to Mitotic Spindles Is Mediated by Phosphorylation on Ser^{558} by Aurora A: A Novel Pharmacodynamic Method for Measuring Aurora A Activity

Patrick J. LeRoy,[1] John J. Hunter,[1] Kara M. Hoar,[1] Krissy E. Burke,[2] Vaishali Shinde,[2] Jason Ruan,[2] Douglas Bowman,[1] Katherine Galvin,[3] and Jeffrey A. Ecsedy[1]

Departments of [1]Molecular and Cellular Oncology, [2]Discovery Technologies, and [3]Cancer Pharmacology, Millennium Pharmaceuticals, Cambridge, Massachusetts

Abstract

Aurora A is a serine/threonine protein kinase essential for normal mitotic progression. Aberrant increased expression of Aurora A, which occurs frequently in human cancers, results in abnormal mitoses leading to chromosome instability and possibly tumorigenesis. Consequently, Aurora A has received considerable attention as a potential target for anticancer therapeutic intervention. Aurora A coordinates several essential mitotic activities through phosphorylation of a variety of proteins, including TACC3, which modulates microtubule stabilization of the mitotic spindle. Recent studies identified a conserved serine in *Xenopus* (Ser^{626}) and *Drosophila* (Ser^{863}) TACC3 orthologues that is phosphorylated by Aurora A. We show that this conserved serine on human TACC3 (Ser^{558}) is also phosphorylated by Aurora A. Moreover, phosphorylation of TACC3 by Aurora A in human cells is essential for its proper localization to centrosomes and proximal mitotic spindles. Inhibition of Aurora A with the selective small molecule inhibitor MLN8054 in cultured human tumor cells resulted in mislocalization of TACC3 away from mitotic spindles in a concentration-dependent manner. Furthermore, oral administration of MLN8054 to nude mice bearing HCT-116 human tumor xenografts caused a dose-dependent mislocalization of TACC3 away from spindle poles that correlated with tumor growth inhibition. As TACC3 localization to mitotic spindles depends on Aurora A–mediated phosphorylation, quantifying TACC3 mislocalization represents a novel pharmacodynamic approach for measuring Aurora A activity in cancer patients treated with inhibitors of Aurora A kinase. [Cancer Res 2007;67(11):5362–70]

Introduction

Aurora A belongs to a highly conserved family of serine/threonine protein kinases that also includes Aurora B and Aurora C. The *Aurora A* gene maps to chromosomal region 20q13.2, which is frequently amplified in a diverse array of human cancers (1–6). Amplification of the *Aurora A* gene is implicated in oncogenesis and tumor progression. For instance, increased Aurora A expression in experimental rodent models induces centrosome amplification, chromosome instability, and aneuploidy, resulting in malignant transformation (6, 7). Moreover, targeted forced expression of Aurora A in the mouse mammary gland induces mitotic abnormalities that precede tumor formation (8, 9).

Aurora A localizes to centrosomes and proximal mitotic spindles where it coordinates essential mitotic activities including centrosome separation, mitotic spindle formation, chromosome alignment, the spindle assembly checkpoint, and cytokinesis (10–15). These distinct activities are orchestrated by Aurora A through its interaction with, and phosphorylation of, a variety of mitotic proteins, including TACC3.

Recent studies identified the conserved residues Ser^{626} of *Xenopus* TACC3 (Maskin) and Ser^{863} of *Drosophila* TACC3 (D-TACC) as the site phosphorylated by Aurora A (16–18). This site is conserved in human TACC3 (Ser^{558}). Localization of TACC proteins to centrosomes was shown to be dependent on phosphorylation by Aurora A in *Caenorhabditis elegans, Xenopus*, and *Drosophila*, and it was proposed that this phosphorylation is required for regulating mitotic spindle pole dynamics and organization (16–20). TACC proteins recruit and form a complex at the centrosomes with the Minispindles (Msps)/XMAP215/ch-TOG (colon and hepatic tumor overexpressing gene) family of microtubule-associated proteins (19, 21–23). In this complex, TACC3 modulates the microtubule stabilizing activity of Msps/XMAP215/ch-TOG. For example, mutant D-TACC in *Drosophila* embryos as well as TACC3-depleted HeLa cells cannot properly localize Msps/ch-TOG to centrosomes, resulting in abnormally short and partially destabilized spindle centrosomal microtubules as well as defects in chromosome congression (21, 22). These mitotic defects lead to an accumulation of cells in the G_2-M cell cycle phases, phenotypes shared by Aurora A inhibition (24, 25).

The oncogenic potential and essential role in mitosis of Aurora A make it an intriguing target for anticancer therapeutic intervention (26, 27). Knockdown of the protein in human tumor cells by RNA interference (RNAi) or inactivation of the kinase using antibody microinjection causes mitotic accumulation and eventual apoptosis (25, 28, 29). MLN8054 (Millennium Pharmaceuticals, Inc.) is the first selective small molecule inhibitor of Aurora A to enter clinical trials in patients with advanced cancers. MLN8054 inhibits proliferation of a diverse group of cultured human tumor cell lines and possesses antitumor activity against human xenografts grown in nude mice (24).

Until now, there have been no reports of direct pharmacodynamic markers for measuring Aurora A inhibition in cancer patients. Although Aurora A inhibition can be monitored through an increased mitotic index, this approach may have limitations as the ensuing mitotic arrest is transient. Moreover, antibody reagents detecting phosphorylated Aurora A substrates may not be sufficiently robust for accurate detection in clinical tumor specimens.

Note: Current address for J.J. Hunter: Department of Preclinical Research, XOMA US (LLC), 2910 Seventh Street, Berkeley, CA 94710.

Requests for reprints: Jeffrey A. Ecsedy, Millennium Pharmaceuticals, Inc., 40 Landsdowne Street, Cambridge, MA 02139. Phone: 617-444-1541; Fax: 617-551-8905; E-mail: jeffrey.ecsedy@mpi.com.

doi:10.1158/0008-5472.CAN-07-0122

Here, we examine TACC3 localization to centrosomes and proximal mitotic spindles as a direct pharmacodynamic measure of Aurora A activity in tumors. Specifically, we show that human Aurora A phosphorylates TACC3 on Ser^{558}. Mutation of this site to an alanine decreases localization of TACC3 to the centrosomes and proximal mitotic spindles in human colon tumor cells. Using MLN8054, we show that inhibition of Aurora A activity in cultured cells prevents proper localization of endogenous TACC3 in a concentration-dependent manner. Furthermore, oral administration of MLN8054 to mice bearing human tumor xenografts also disrupted TACC3 localization in tumor sections. In summary, this work introduces a novel pharmacodynamic method for measuring Aurora A activity by quantifying the loss of TACC3 from centrosomes and proximal mitotic spindles.

Materials and Methods

Mammalian and bacterial expression vectors. TACC3 (amino acids 331–838) was cloned into the bacterial expression vector pDest15 (Invitrogen) containing an NH_2-terminal glutathione *S*-transferase (GST) fusion. The product of this construct was expressed in *Escherichia coli* and is referred to as GST-ΔTACC3. Serine to alanine mutations in residues 399, 402, and 558 in various combinations were generated by site-directed mutagenesis. Full-length TACC3 was cloned into the mammalian retroviral expression vector pLNCX (BD Biosciences) containing an NH_2-terminal enhanced green fluorescent protein (EGFP) tag (pLNCX/EGFP-WT TACC3). A serine to alanine mutation in residue 558 of TACC3 was generated by site-directed mutagenesis (pLNCX/EGFP-MUT TACC3).

***In vitro* kinase assay.** Recombinant Aurora A (100 ng) prepared as described previously (24) was incubated in kinase buffer [20 mmol/L HEPES (pH 7.5), 5 mmol/L $MgCl_2$, 10 μmol/L ATP] and 10 μCi γ-[^{32}P]ATP alone or in the presence of various substrates, including 2 μg of bacterially expressed GST-ΔTACC3 (wild type or Ser^{399}, Ser^{402}, and Ser^{558} to alanine mutants in various combinations), GST-cyclin B1, and histone H1 (Upstate Biotechnology) for 30 min at room temperature. The reactions were stopped by the addition of NuPAGE SDS sample buffer (Invitrogen), and the proteins were resolved by SDS-PAGE. Labeled proteins were visualized by autoradiography.

Identification of TACC3 phosphorylated residues. Purified GST-ΔTACC3 (30 μg) was incubated in kinase buffer [20 mmol/L HEPES (pH 7.5), 5 mmol/L $MgCl_2$, 100 μmol/L ATP] alone or in the presence of recombinant Aurora A (1.5 μg) for 30 min at room temperature. The reactions were stopped, and TACC3 phosphorylated residues were identified by liquid chromatography tandem mass spectrometry (LC-MS/MS) as previously described (30).

EGFP-WT TACC3 and EGFP-MUT TACC3 stable cells. To generate retrovirus, 1.5×10^6 293-EBNA cells (Invitrogen) grown on 10-cm tissue culture dishes were cotransfected with 2 μg pLNCX/EGFP-WT TACC3 or pLNCX/EGFP-MUT TACC3 with 2 μg pN8ε-VSV-G and 2 μg pN8ε-gag-pol. Preparation of the pN8ε-VSV-G and pN8ε-gag-pol vectors was previously described (31). Transfections were done using LipofectAMINE reagent according to the manufacturer's recommended methods (Invitrogen). Viral supernatants were harvested every 24 h for 72 h, passed through a 0.45-μm filter (Pall Gelman Laboratories), and stored at −80°C. For infection into HCT-116 cells (obtained from the American Type Culture Collection), viruses were diluted 1:1 in McCoy's Modified 5A media (Invitrogen) supplemented with 2 mmol/L L-glutamine (Invitrogen), 10% fetal bovine serum (Hyclone), and 8 μg/mL polybrene (Sigma). Following three 12-h rounds of transduction, stable expressing pools were selected with 500 μg/mL G418. Wild-type pools are referred to as EGFP-WT TACC3, and Ser^{558} to Ala mutant pools are referred to as EGFP-MUT TACC3. Stable pools (2×10^5 cells) were grown on glass coverslips (18 × 18 × 1.5 mm, VWR) in six-well tissue culture dishes in McCoy's Modified 5A media supplemented with 2 mmol/L L-glutamine and 10% fetal bovine serum for 38 h. DMSO (0.2%) or MLN8054 (1 μmol/L) were added for 2 h, and cells were fixed with 4% paraformaldehyde (Electron Microscopy Sciences) followed by incubation with Hoechst 33321 (1:5,000; Molecular Probes) in PBS for 30 min. Cells were washed twice in PBS and mounted onto glass slides with Fluoromount G (Electron Microscopy Sciences). Cells were visualized with a LSM 5 Pascal Laser Scanning Confocal microscope (Zeiss), and images were processed using Metamorph Version 6.3R7 (Molecular Devices).

Immunoblotting. HCT-116, EGFP-WT TACC3, and EGFP-MUT TACC3 cells were lysed in NP40 buffer [50 mmol/L HEPES (pH 7.6), 150 mmol/L NaCl, 1 mmol/L EDTA, 5% glycerol, 1% NP40] containing phosphatase and protease inhibitors (5 mmol/L NaF, 1 mmol/L Na_3VO_4, 1× Protease Inhibitor Cocktail Set; Calbiochem). The lysates were clarified by centrifugation at 15,000 rpm for 15 min and denatured by heating to 100°C in NuPAGE SDS sample buffer. Proteins were resolved by SDS-PAGE, Western blotted, and detected with the ECL Western Blotting Detection System (Amersham Biosciences). Primary antibodies used for Western blotting included anti-TACC3 rabbit antibody (1:1,000; Santa Cruz, H300) and anti-β-actin mouse antibody (1:10,000; Abcam). The secondary antibodies used were sheep anti-mouse IgG horseradish peroxidase–linked whole antibody (1:2,500; Amersham) and donkey anti-rabbit IgG horseradish peroxidase–linked whole antibody (1:2,500; Amersham).

Immunofluorescence. HCT-116 cells grown on glass coverslips as described above were treated with DMSO (0.2%) or MLN8054 (1 μmol/L) for 4 h followed by 100 nmol/L bortezomib (VELCADE; Millennium Pharmaceuticals) for the last 2 h. Bortezomib inhibits the proteosome, thereby blocking mitotic cells at the metaphase to anaphase transition. Cells were fixed with 4% paraformaldehyde and permeabilized with 0.5% Triton X-100 in PBS. Blocking Reagent (Roche) was added to cells for 30 min followed by 1 h of incubation with the primary antibody in Blocking Reagent. Cells were washed in PBS and in PBS containing 0.05% Tween followed by addition of the secondary antibody in Blocking Reagent for 1 h. Cells were washed with PBS and Hoeschst 33321 in PBS (1:10,000; Molecular Probes) was added for 5 min. Primary antibodies included anti-TACC3 rabbit antibody (1:1,000), anti–Ipl1- and aurora-related kinase 1 (IAK1) mouse monoclonal antibody (1:75; BD Biosciences PharMingen), anti-NuMA mouse antibody (1:100; Calbiochem, Ab-2 107-7), anti-α-tubulin (1:500; Sigma, clone DM1A), and anti–phosphorylated Aurora A Thr^{288} (Aurora A pThr^{288}; 1:100, Millennium Pharmaceuticals). Secondary antibodies included Alexa 488–conjugated goat anti-rabbit IgG (1:250; Molecular Probes) and Alexa 594–conjugated goat anti-mouse IgG (1:250; Molecular Probes). Immunofluorescently labeled cells were visualized, and images were processed as described above.

TACC3 localization assay. HCT-116 or HT29 cells (obtained from the American Type Culture Collection) were grown on 96-well tissue culture dishes (2.5×10^3 per well) for 40 h in McCoy's Modified 5A media (Invitrogen) supplemented with 2 mmol/L L-glutamine (Invitrogen) and 10% fetal bovine serum (Hyclone). Compounds were added to cells in 2-fold serial dilution, and cells were incubated in a 37°C humidified cell culture chamber for 2.5 h. Compounds at each dilution were added as replicates in three rows on the dish. Cells treated with DMSO ($n = 3$ wells per plate; 0.2% final concentration) served as the vehicle control. After treatment, cells were fixed with 4% paraformaldehyde and permeated with 0.5% Triton X-100. The cells were treated with Blocking Reagent (Roche) for 20 min and were then stained with anti-TACC3 rabbit antibody (1:1,000) and anti-IAK1 mouse monoclonal antibody (1:75) in Blocking Reagent followed by Alexa 488–conjugated goat anti-rabbit IgG (1:250), Alexa 594–conjugated goat anti-mouse IgG (1:250), and Hoechst 33321 (1:5,000) in Blocking Reagent. The cells were visualized using a Discovery-1 High Content Imaging System (Molecular Devices). Images from nine sites per well were collected at ×20 magnification. Five *Z*-sections were acquired at 2-μm increments and were compressed to single images at each site using Metamorph Version 6.3R7 (Molecular Devices) to ensure that all fluorescent structures throughout the volume of each cell were captured. TACC3 intensity maps (Fig. 4) were generated by computing TACC3 fluorescent intensity within the indicated areas using ProGuru. ProGuru is a software program developed at Millennium Pharmaceuticals designed for custom quantitative high-content image analysis and visualization. TACC3 localization to the centrosomes was determined by measuring TACC3 fluorescent intensity within IAK1 immunopositive centrosomes using ProGuru software (Fig. 5).

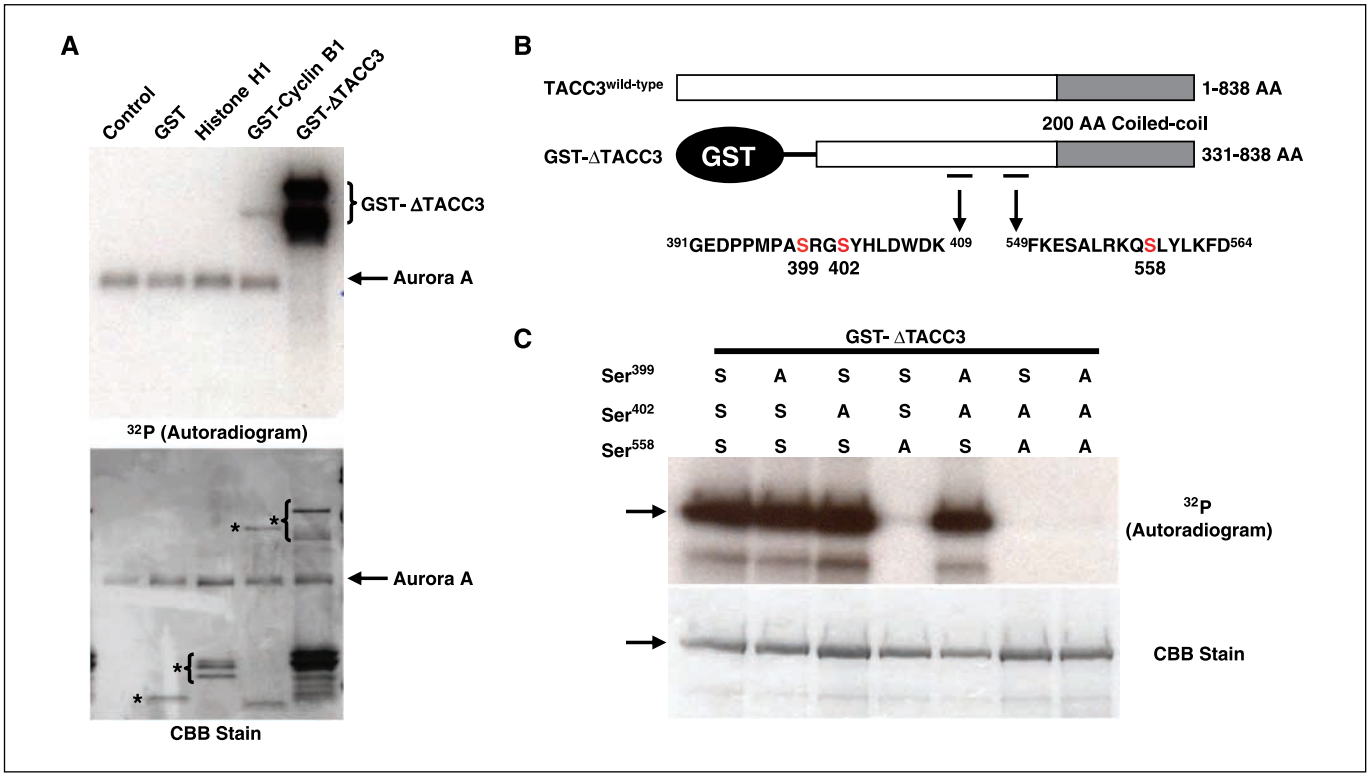

Figure 1. Aurora A phosphorylates TACC3 on Ser^{558}. *A,* recombinant Aurora A was incubated in an *in vitro* kinase assay alone (control) or with GST, histone H1, GST-fused cyclin B1, or GST-ΔTACC3 (GST fused to TACC3 amino acids 331–838). ^{32}P autoradiogram (*top*) and Coomassie brilliant blue (*CBB*)–stained gel (*bottom*). *, migration of the indicated substrate within each lane. *B,* GST-ΔTACC3 residues phosphorylated by Aurora A in an *in vitro* kinase assay were identified by LC-MS/MS. The amino acid sequences indicate tryptic peptides containing phosphorylated residues upon Aurora A phosphorylation. Phosphorylated residues (*red*). *Numbers,* amino acid sequence of wild-type TACC3. *C,* Ser^{399}, Ser^{402}, and Ser^{558} of GST-ΔTACC3 were mutated to alanine in various combinations and incubated with Aurora A in an *in vitro* kinase assay. *S,* serine at the indicated residue; *A,* alanine at the indicated residue. ^{32}P autoradiogram (*top*) and Coomassie brilliant blue–stained gel (*bottom*).

Concentration response curves were generated by calculating the decrease of TACC3 fluorescent intensity within centrosomes of compound-treated samples relative to the DMSO-treated controls; IC_{50} values were determined from those curves.

Generation of Aurora A pThr^{288} antibodies. A peptide containing the Aurora A pThr^{288} residue (H2N-CPSSRRT-pT-LCGTLD-OH; New England Peptide) was coupled to keyhole limpet hemocyanin (Pierce) and used to immunize rabbits (Epitomics). Hybridomas were generated in collaboration with Epitomics. Antibodies were affinity purified from hybridoma supernatants using Protein A-Sepharose (Rockland Immunochemicals).

Aurora A pThr^{288} autophosphorylation assay. The Aurora A pThr^{288} autophosphorylation assay was done as previously described (24). HeLa cells (obtained from the American Type Culture Collection) were grown on 96-well dishes (1.8×10^4 per well) for 18 to 20 h in DMEM (Invitrogen) supplemented with 2 mmol/L L-glutamine and 10% fetal bovine serum. Compounds were added to the cells in 2-fold serial dilutions, and cells were incubated in a 37°C humidified cell culture chamber for 60 min. Compounds at each dilution were added as replicates in four rows on the dish. Cells treated with DMSO (n = 8 wells per plate; 0.2% final concentration) served as the vehicle control. The cells were then fixed with 4% paraformaldehyde in PBS for 10 min, permeated with 0.5% Triton X-100 in PBS for 10 min, and washed twice in PBS. Fixed cells were treated with Blocking Reagent (Roche) for 20 min at room temperature and stained for 90 min at room temperature with anti-pThr^{288} rabbit monoclonal antibody (1:200; Millennium Pharmaceuticals) and anti–phosphorylated Ser/Thr-Pro, MPM2 mouse antibody (1:750; Upstate Biotechnology) in Blocking Reagent. The cells were washed twice with PBS and once with 0.05% Tween 20 in PBS and stained for 45 min at room temperature with Alexa 488–conjugated goat anti-rabbit IgG (1:180) and Alexa 594–conjugated chicken anti-mouse IgG (1:180; Molecular Probes) in Blocking Reagent. The cells were then washed twice with PBS and stained for 30 min at room temperature with Alexa 488–conjugated chicken anti-goat IgG (1:180; Molecular Probes) in Blocking Reagent. The cells were washed once with PBS, stained with Hoescht (1:10,000) for 5 min, and washed twice in PBS. Immunofluorescent cells were visualized using a Discovery-1 High Content Imaging System. Images from 16 sites per well were captured with a ×20 objective lens. Inhibition of Aurora A was determined by measuring pThr^{288} (Aurora A autophosphorylation) fluorescent intensity within MPM2-immunopositive (mitotic) cells using Metamorph version 6.3R7. Concentration-response curves were generated by calculating the decrease of pThr^{288} fluorescent intensity in compound-treated samples relative to the untreated controls.

***In vivo* immunofluorescence.** Treatment of mice bearing HCT-116 tumor xenografts with varying doses of MLN8054 was done as previously described (24). Formalin-fixed, paraffin-embedded HCT-116 tumor sections (5 μm) were processed using two different methods. Sections stained for TACC3 and NuMA were processed using the Discovery XT (Ventana Medical Systems) automated slide preparation instrument. Sections were deparaffinized on the instrument with EZ prep solution, and antigen retrieval was completed with Cell Conditioning 1 solution (CC1, Ventana Medical Systems). Sections stained for Aurora A pThr^{288} and MPM2 (anti–phosphorylated Ser/Thr-Pro mouse antibody; Upstate Biotechnology) were deparaffinized with xylene and hydrated with ethanol washes. Antigen retrieval was completed with 0.01 mol/L citrate buffer (pH 6.0) solution with a pressure cooker as the heating source. Sections were stained with anti-TACC3 rabbit antibody (1:100) and anti-NuMA mouse antibody (1:20), or anti–phosphoryalted Aurora A Thr^{288} (1:8) and MPM2 antibody (1:100). Secondary antibodies used included Rhodamine Red-X-AffiniPure goat

anti-rabbit IgG (1:25; Jackson ImmunoResearch) and Alexa 488–conjugated goat anti-mouse IgG (1:50; Molecular Probes) or 568-streptavidin–conjugated secondary (1:300; Molecular Probes) and Alexa Fluor 488–conjugated goat anti-mouse IgG (1:500; Molecular Probes) antibodies, respectively. Slides were washed in PBS and mounted with 4′,6-diamidino-2-phenylindole Vectashield Hard Set Medium (Vector). Images were captured using a Nikon Eclipse E800 microscope (×40 objective) and processed using Metamorph version 6.3R7.

Results

TACC3 is phosphorylated on Ser^{558} by Aurora A *in vitro*. To identify residues on human TACC3 phosphorylated by Aurora A, *in vitro* kinase assays were done. Aurora A robustly phosphorylated GST-ΔTACC3 (TACC3 amino acids 331–838 fused to NH_2-terminal GST; Fig. 1*A, autoradiogram*). Expression of GST-ΔTACC3 resulted in a number of degradation products (Fig. 1*A, CBB stain*), some which were phosphorylated by Aurora A in this assay. Low or undetectable levels of phosphorylation were detected when Aurora A was incubated with GST alone, histone H1, or GST-fused to cyclin B1. Aurora A also underwent detectable autophosphorylation except in the presence of GST-ΔTACC3, which may have been due to the reaction stoichiometry favoring TACC3 as a substrate.

Microcapillary LC-MS/MS was used to identify phosphorylated TACC3 residues from GST-ΔTACC3 phosphorylated *in vitro* by Aurora A. Three phosphorylated residues were identified by this method: Ser^{399}, Ser^{402}, and Ser^{558} (Fig. 1*B*). To confirm that Aurora A phosphorylated TACC3 on these serines, GST-ΔTACC3 containing serine to alanine mutations in these residues in various combinations were used as substrates in an *in vitro* kinase assay with Aurora A (Fig. 1*C*). Radiolabeling of GST-ΔTACC3 containing Ser^{399}Ala or Ser^{402}Ala mutations was similar to that of wild-type GST-ΔTACC3, indicating that the identification of these residues as putative Aurora A phosphorylation sites may have been an artifact of MS analysis. Radiolabeling was not detected in any GST-ΔTACC3 containing Ser^{558}Ala mutations. Therefore, we conclude that Aurora A phosphorylated GST-ΔTACC3 on Ser^{558}. This was consistent with previous studies showing that Aurora A phosphorylates *Drosophila* and *Xenopus* TACC3 on a conserved residue corresponding to mammalian TACC3 Ser^{558} (16, 17, 32).

Proper TACC3 localization is dependent on Aurora A–mediated phosphorylation of Ser^{558}. To determine whether phosphorylation of Ser^{558} is required to target human TACC3 to the mitotic spindle, the localization of exogenously expressed EGFP-WT TACC3 (wild-type, full-length TACC3 fused to NH_2-terminal EGFP) and EGFP-MUT TACC3 (Ser^{558}Ala, full-length TACC3 fused to NH_2-terminal EGFP) were compared in HCT-116 cells (Fig. 2*A*). Western blots showed that EGFP-WT TACC3 and EGFP-MUT TACC3 clones expressed equal levels of protein (Fig. 2*B*). EGFP-WT TACC3 localized primarily to mitotic spindles in prometaphase/metaphase cells, whereas EGFP-MUT TACC3 did not fully localize to apparent mitotic spindles and displayed a diffuse staining throughout mitotic cells. Aurora A inhibition with the selective small molecule inhibitor MLN8054 resulted in EGFP-WT TACC3 redistribution away from the mitotic spindle, mirroring the localization of EGFP-MUT TACC3. Previous studies showed that Aurora A inhibition with MLN8054 allowed for the formation of a mitotic spindle, albeit abnormal (24). We infer from these findings that complete TACC3 localization to the mitotic spindle is dependent on Ser^{558} phosphorylation by Aurora A.

Localization of endogenous TACC3 was also evaluated in HCT-116 cells treated with 1 μmol/L MLN8054 for 4 h followed by bortezomib for the last 2 h before fixation to trap mitotic cells immediately before anaphase onset. This allowed for the observation of MLN8054 treated and untreated cells at a similar stage of mitosis. Cells were fixed and stained for mitotic spindles, centrosomes, and spindle poles using antibodies directed against α-tubulin, Aurora A, and NuMA, respectively (Fig. 3). Similar to the EGFP-WT TACC3 overexpressing clones, TACC3 did not fully localize to mitotic spindles in the presence of MLN8054 and displayed a diffuse staining throughout mitotic cells, even when a bipolar spindle formed (Fig. 3*A*). Typically, MLN8054 results in abnormal mitotic spindle formation accompanied by chromosome congression defects (24). TACC3 localizes to centrosomes and proximal mitotic spindles (33); therefore, colocalization with the

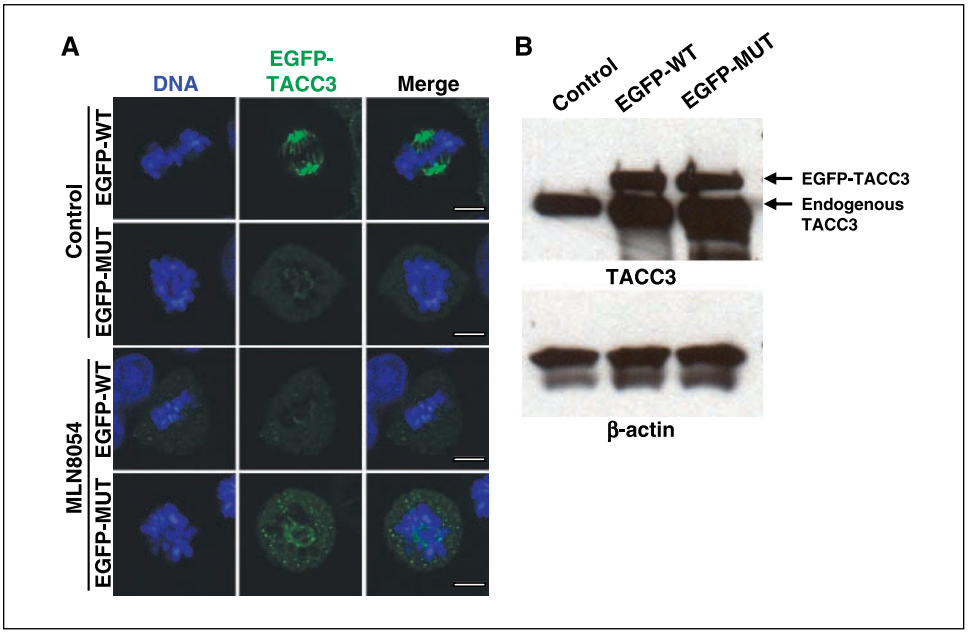

Figure 2. TACC3 localization to mitotic spindles is dependent on Ser^{558} phosphorylation and Aurora A activity. *A,* representative immunofluorescent images of mitotic HCT-116 cells constitutively expressing EGFP fused to wild-type TACC3 (EGFP-WT) or TACC3 containing a Ser^{558} to alanine mutation (EGFP-MUT; *green*) and stained with Hoechst (DNA, *blue*). Cells were treated with DMSO (control) or 1 μmol/L MLN8054 for 2 h. Overlapping green and blue images (*Merge*). *Bar,* 5 μm. *B,* Western blot of HCT-116 cells, untransfected (control) or constitutively expressing EGFP-WT TACC3 or EGFP-MUT TACC3 probed for TACC3 (*top*) and β-actin (*bottom*), which served as a protein loading control.

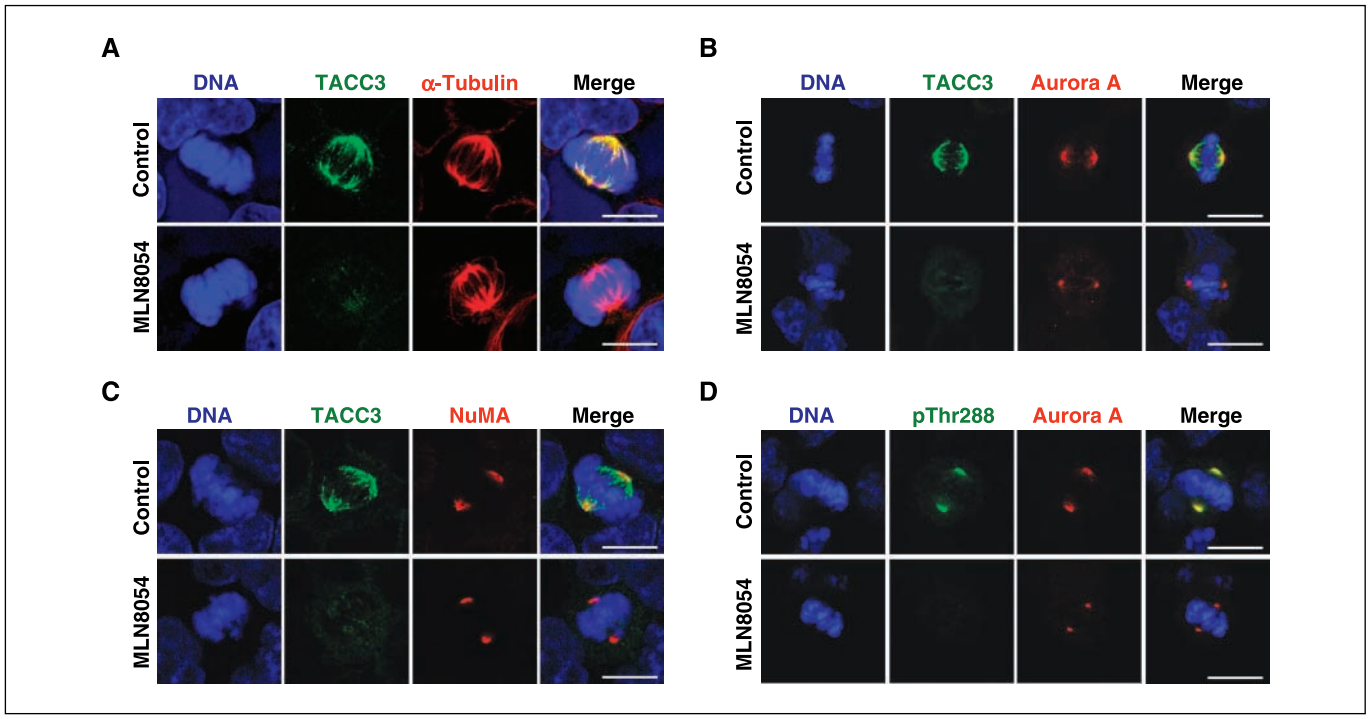

Figure 3. HCT-116 cells were treated with DMSO (control) or 1 μmol/L MLN8054 for 4 h. Bortezomib (100 nmol/L) was added for the final 2 h to arrest mitotic cells at the metaphase to anaphase transition. Representative immunofluorescent images of mitotic cells stained with anti-TACC3 (*green*) and anti-α-tubulin (*red*) antibodies (*A*), anti-TACC3 (*green*) and anti–Aurora A (*red*) antibodies (*B*), anti-TACC3 (*green*) and anti-NuMA (*red*) antibodies (*C*), or anti–Aurora A pThr^{288} (*green*) and anti–Aurora A (*red*) antibodies (*D*). All images were also stained with Hoechst (DNA, *blue*). Merged images are shown. *Bar,* 10 μm.

centrosomal protein Aurora A and the spindle pole protein NuMA was examined (Fig. 3*B* and *C*, respectively). Although both Aurora A and NuMA were properly localized in these cells, there was no significant colocalization with TACC3 in cells treated with MLN8054. To ensure that Aurora A activity was inhibited in these cells, autophosphorylation on Thr^{288} (pThr^{288}) was assessed (Fig. 3*D*). DMSO-treated HCT-116 cells exhibited detectable pThr^{288}, which colocalized with total Aurora A. In MLN8054-treated cells,

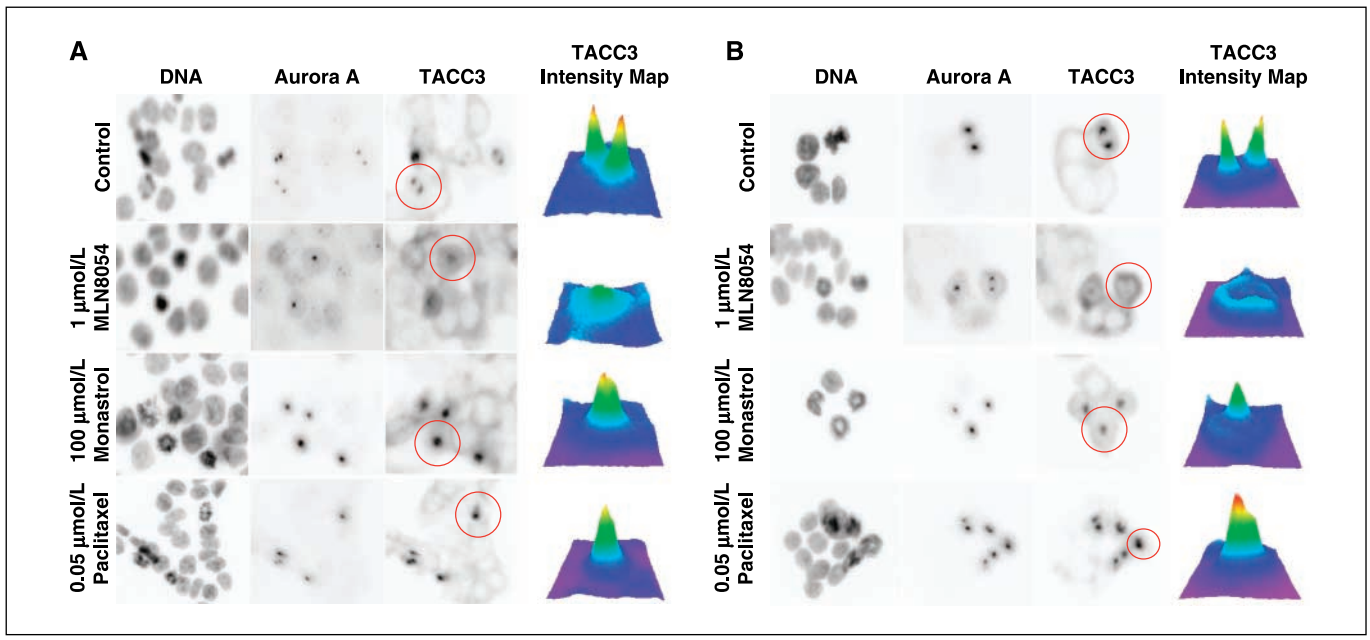

Figure 4. MLN8054 mislocalizes TACC3 away from centrosomes in cultured cells. HCT-116 (*A*) and HT29 (*B*) cells were treated with DMSO, 1 μmol/L MLN8054, 100 μmol/L monastrol, or 0.025 μmol/L paclitaxel for 2.5 h. Cells were stained with Hoechst (DNA), anti–Aurora A mouse antibody (Aurora A), and anti-TACC3 rabbit antibody (TACC3) and imaged using a Discovery-1 High Content Imaging System. Using ProGuru Software, TACC3 intensity maps were generated by computing TACC3 fluorescent intensity of the cells encompassed by the red circles present in the TACC3 images. All TACC3 images and TACC3 intensity maps were generated using the same intensity scale.

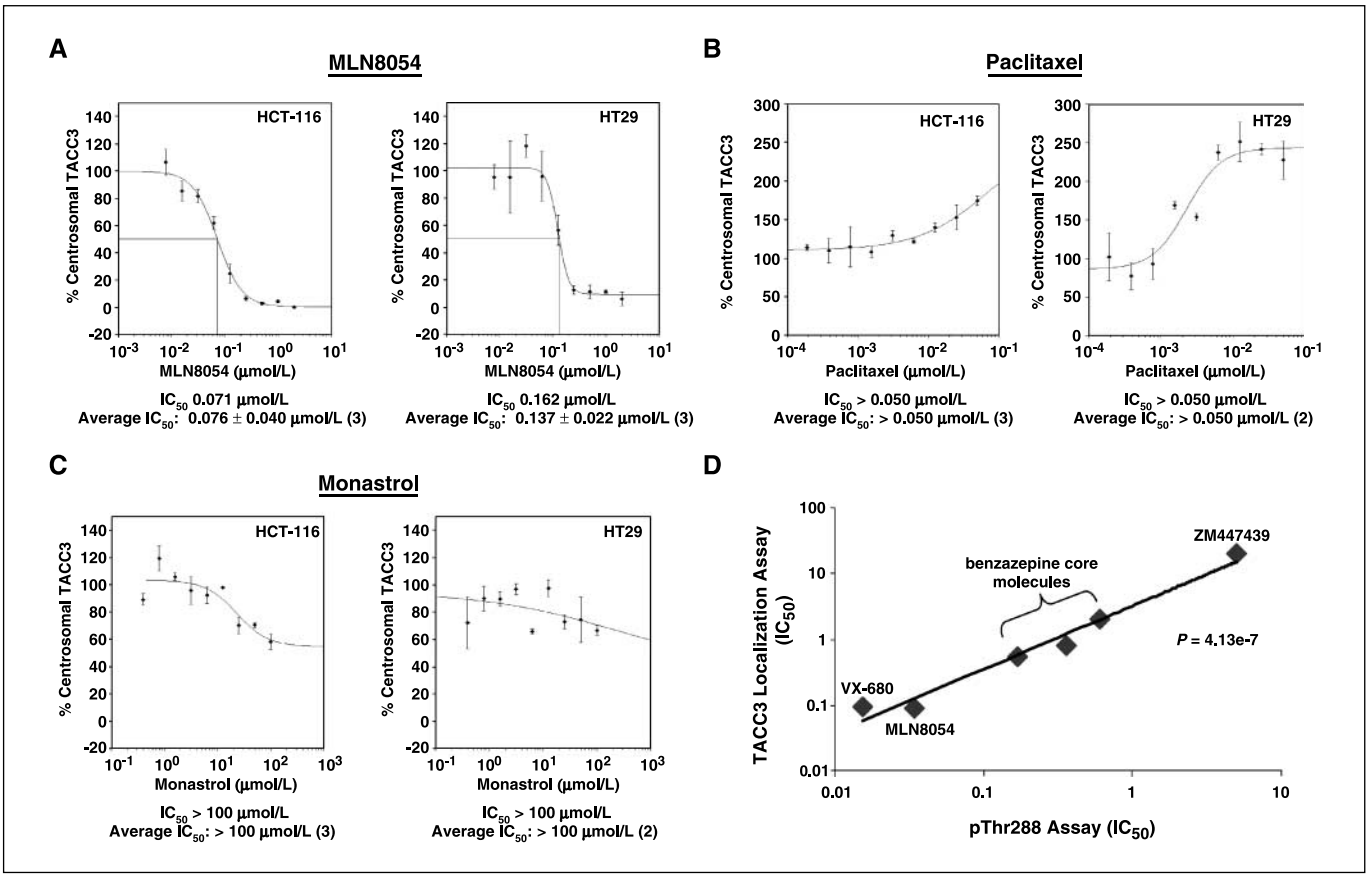

Figure 5. TACC3 localization assay. TACC3 localization to centrosomes was measured in HCT-116 and HT29 cells in the presence of MLN8054 (*A*), paclitaxel (*B*), and monastrol (*C*). The concentration-response curves were generated by calculating the decrease of TACC3 fluorescent intensity in centrosomes (defined by Aurora A localization) in treated samples relative to the DMSO-treated controls. *Points,* averages of three replicate samples; *bars,* SD. Bisecting lines in reflect compound concentration necessary to achieve 50% inhibition relative to controls (IC_{50} values). The IC_{50} number was calculated from the curves shown. Average IC_{50} numbers represent the average $IC_{50} \pm$ SD derived from multiple experiments, indicated by the number in parentheses. *D,* comparison of IC_{50}s for six inhibitors, including MLN8054, MLN8054-related compounds sharing the benzezapine core scaffold, VX-680, and ZM447439, generated in the TACC3 localization assay and in the Aurora A $pThr^{288}$ autophosphorylation assay. The correlation coefficient (*P*) is shown.

$pThr^{288}$ was not detected, although total Aurora A remained, showing that Aurora A activity was inhibited in these cells. These results show that proper localization of endogenous TACC3 during mitosis is dependent on Aurora A activity.

MLN8054 mislocalizes TACC3 away from centrosomes in a concentration-dependent manner. TACC3 localization was quantified by measuring TACC3 immunofluorescent intensity in Aurora A–positive HCT-116 and HT29 mitotic cells treated with MLN8054 (Fig. 4). In control treated samples, TACC3 robustly localized to distinct poles in both cell lines as indicated by the TACC3 intensity maps. However, MLN8054 caused TACC3 to be diffusely localized throughout mitotic cells. As MLN8054 leads to a mitotic spindle defects (24), other inhibitors that affect mitotic spindle formation independent of Aurora A activity were also examined. These included monastrol and paclitaxel. Although both inhibitors resulted in spindle defects, TACC3 localization remained focused within mitotic cells.

A cell-based assay was developed to quantify TACC3 localization to Aurora A–positive spots within HCT-116 and HT29 mitotic cells treated with various concentrations of MLN8054, paclitaxel, and monastrol (Fig. 5). TACC3 immunofluorescent intensity was measured by automated fluorescent microscopy and was quantified using ProGuru image analysis software. MLN8054 inhibited TACC3 localization with an IC_{50} of 0.076 ± 0.040 μmol/L in HCT-116 cells and 0.137 ± 0.020 μmol/L in HT29 cells. Neither paclitaxel nor monastrol sufficiently inhibited TACC3 localization to achieve an IC_{50} value in either cell line. In fact, increasing concentrations of paclitaxel amplified TACC3 localization to Aurora A–positive spots in mitotic cells in both cell lines. Monastrol slightly diminished TACC3 localization to Aurora A–positive spots, although not sufficiently to generate IC_{50} values.

To determine how well TACC3 mislocalization predicted Aurora A activity, IC_{50} values for six inhibitors generated in the TACC3 localization assay were compared with those generated in the Aurora A $pThr^{288}$ autophosphorylation assay (Fig. 5*D*). This latter assay quantifies the immunofluorescent intensity of Aurora A $pThr^{288}$ as a measure of kinase activity (24). There was a strong correlation between IC_{50} values generated between these two assays for inhibitors of different structural classes. These included MLN8054; three MLN8054-related molecules sharing the benzazepine core scaffold (24); VX-680, a dual Aurora A and Aurora B inhibitor (34); and ZM447439, an Aurora B selective inhibitor (35, 36). Collectively, these experiments suggest that TACC3 localization can be used to measure Aurora A activity in mitotic cells.

MLN8054-mediated Aurora A inhibition mislocalizes TACC3 in human tumor xenografts. The quantitative mislocalization of

TACC3 from centrosomes presents a potential for use as a pharmacodynamic marker of Aurora A activity *in vivo*. To assess this possibility, nude mice bearing HCT-116 tumor xenografts were treated with a single oral dose of MLN8054 at 3, 10, 30, or 60 mg/kg, and tumors were collected 8 h later. Tumor sections were costained for TACC3, NuMA, and DNA (Fig. 6*A*). In vehicle-treated samples, NuMA localized to opposing spindle poles, and TACC3 localized to the mitotic spindle. A similar localization was found in metaphase cells from tumors treated with 3 and 10 mg/kg MLN8054. However, with higher doses of MLN8054 (30 and 60 mg/kg), TACC3 was not readily apparent in metaphase cells. Localization of TACC3 to NuMA-positive mitotic cells was quantified in each dose group (Fig. 6*B*). MLN8054 at 3 and 10 mg/kg induced a slight decrease in properly localized TACC3 in NuMA-positive mitotic cells, although this difference did not achieve statistical significance. However, MLN8054 at 30 and 60 mg/kg caused a robust decrease in spindle-focused TACC3. The dose-dependent loss of TACC3 at spindle poles paralleled the loss of Aurora A autophosphorylation on Thr^{288}, indicating that TACC3 mislocalization directly reflects decreased Aurora A activity in tumors (Fig. 6*C*). Moreover, the dose-dependent loss of TACC3 at spindle poles correlated with previous observations from a separate efficacy study showing a

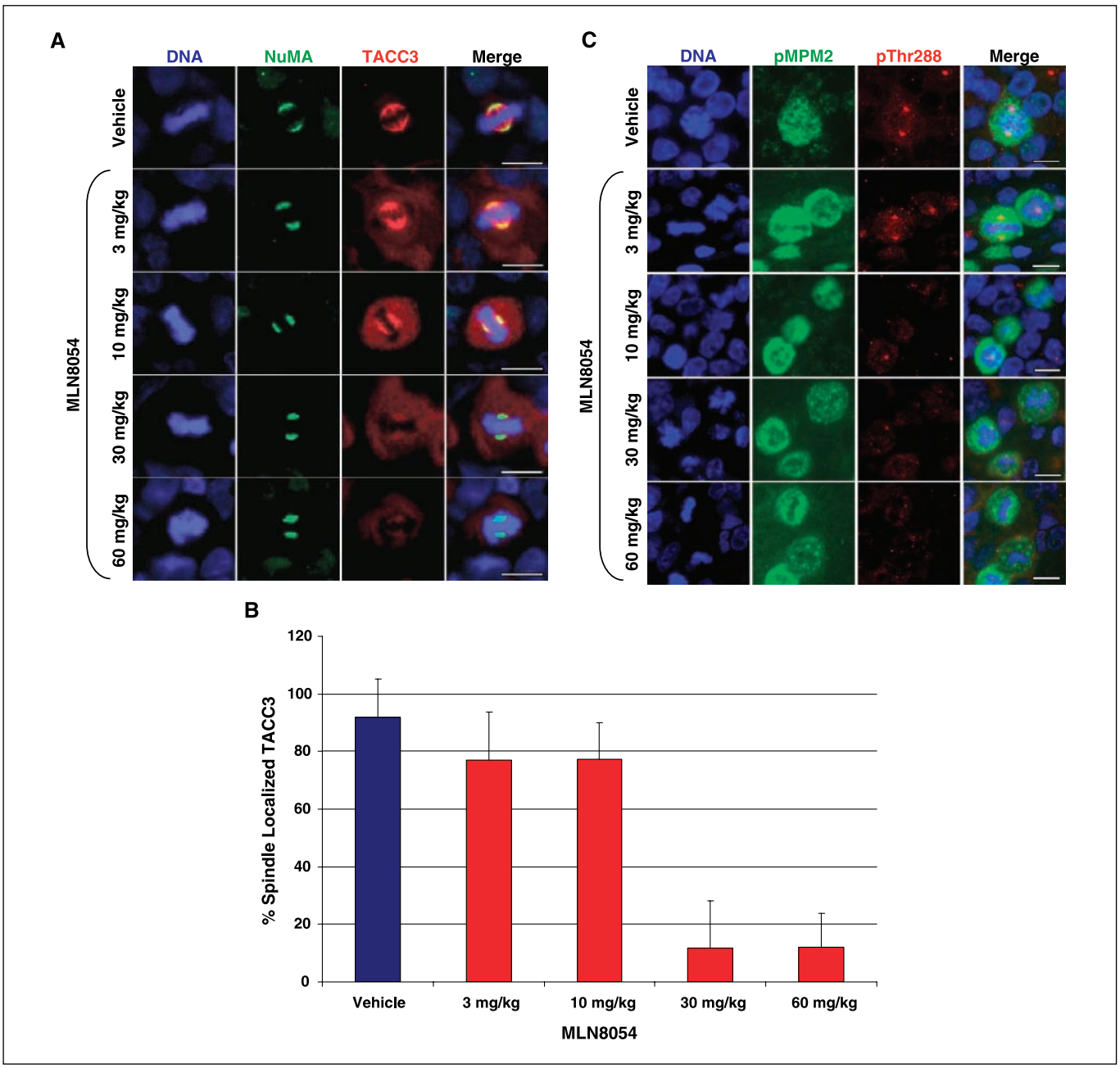

Figure 6. MLN8054 mislocalizes TACC3 away from centrosomes in human tumor xenografts. HCT-116 tumor bearing mice were treated with vehicle or MLN8054 at 3, 10, 30, and 60 mg/kg for 8 h. *A,* representative images from tumor sections stained with anti-NuMA mouse antibody (*green*), anti-TACC3 rabbit antibody (*red*), and Hoechst (DNA, *blue*). *B,* the percentage of mitotic spindles with detectable TACC3 in tumors derived from vehicle and MLN8054-treated animals. *C,* representative images from tumor sections stained with MPM2 antibody (*green*), anti–Aurora A $pThr^{288}$ antibody (*red*), and Hoechst (DNA, *blue*). *Bar,* 10 μm.

partial tumor growth inhibition with 3 or 10 mg/kg once a day oral dose of MLN8054 for 21 days and a maximal tumor growth inhibition with a 30 mg/kg oral dose of MLN8054 (24). Collectively, these results suggest that loss of mitotic spindle-focused TACC3 can be used as a pharmacodynamic measure of Aurora A activity *in vivo*.

Discussion

The Aurora-related kinases have generated significant interest as potential targets for anticancer therapeutic intervention. Towards this end, Millennium Pharmaceuticals developed a selective small molecule Aurora A inhibitor (MLN8054) that entered clinical trials in patients with advanced cancers. In this work, we propose a novel pharmacodynamic method for measuring Aurora A activity in tumors by quantifying TACC3 localization to mitotic spindles. We show that human Aurora A phosphorylates TACC3 on Ser^{558}, and that this phosphorylation is required for TACC3 localization to mitotic spindles. Inactivation of Aurora A in cells using MLN8054 disrupts TACC3 localization to centrosomes in a concentration-dependent manner. In human tumor xenografts, MLN8054 also caused a dose-dependent mislocalization of TACC3 away from spindle poles. As TACC3 localization to mitotic spindles is strictly dependent on Aurora A activity, proper TACC3 localization will likely be a useful pharmacodynamic marker in tumors from cancer patients treated with inhibitors of Aurora A kinase.

Ser^{34}, Ser^{552}, and Ser^{558} of human TACC3 loosely fit within the predicted Aurora A phosphorylation consensus site [KR]X[TS][ILV] (37). These residues are conserved in the *Xenopus* TACC3 orthologue Maskin (Ser^{33}, Ser^{620}, and Ser^{626}), whereas only Ser^{558} is obviously conserved in the *Drosophila* TACC3 orthologue D-TACC (Ser^{863}). Using GST-ΔTACC3 as a substrate in an *in vitro* kinase assay, Ser^{399}, Ser^{402}, and Ser^{558} were identified as potential Aurora A phosphorylated residues by LC-MS/MS phosphomapping. Of these, only Ser^{558} was confirmed to be phosphorylated using various combinations of serine to alanine mutations for each of these residues in GST-ΔTACC3. The conserved Ser^{558} sites on *Xenopus* Maskin (Ser^{626}) and *Drosophila* D-TACC (Ser^{863}) were also previously shown to be phosphorylated by Aurora A (16–18). However, in *Xenopus*, Aurora A also phosphorylated Maskin on Ser^{33} and Ser^{620} (17, 18), whereas in our system, Ser^{552} was not phosphorylated by Aurora A, and Ser^{34} was not present on the GST-ΔTACC3 substrate.

Localization of TACC proteins to centrosomes has been shown in several models to be dependent on Aurora A activity (16–20). For example, knockdown of Aurora A by RNAi or immunodepletion in *C. elegans* embryos, *Xenopus* egg extracts, or *Drosophila* cultured neuroblasts mislocalized TAC-1, Maskin, and D-TACC, respectively, away from centrosomes (18–20). Moreover, in *Drosophila* embryos, GFP-conjugated wild-type D-TACC localized to centrosomes more intensely than did a Ser^{863} to a leucine mutant protein (16). These results are consistent with our findings showing that exogenously expressed EGFP-MUT TACC3 did not fully localize to the mitotic spindle relative to EGFP-WT TACC3. Interestingly, we found that inhibition of Aurora A with MLN8054 mislocalized EGFP-WT TACC3 away from mitotic spindles to a degree similar to that of untreated EGFP-MUT TACC3. These results indicate that Ser^{558} is likely the predominant site of TACC3 that requires phosphorylation by Aurora A for mitotic spindle localization in human cells.

To determine if TACC3 mislocalization could be used to measure inhibition of Aurora A activity, a cell-based TACC3 localization assay was developed to quantify TACC3 localization to centrosomes. Treatment of two colon tumor cell lines with MLN8054 resulted in a concentration-dependent decrease in TACC3 at centrosomes. Moreover, there was a striking correlation in calculated IC_{50}s between the TACC3 localization assay and the Aurora A $pThr^{288}$ autophosphorylation assay for several classes of Aurora inhibitors, indicating that proper TACC3 localization can in fact be used as a measure of Aurora A activity. This effect was not related to general spindle formation defects resulting from Aurora A inhibition, as treatment with other microtubule disrupters, including paclitaxel and monastrol, did not significantly decrease TACC3 localization to centrosomes.

Similar to what was found in cultured tumor cells, HCT-116 tumor xenografts in nude mice also showed a dose-dependent decrease in TACC3 localization to mitotic spindles. This result was similar to what was observed with Aurora A $pThr^{288}$ staining in these samples. However, $pThr^{288}$ staining is often faint and more subject to nonspecific staining in formalin-fixed, paraffin-embedded tissues. Furthermore, Aurora A predominantly localizes to centrosomes, and these small structures are often absent from the plane of section. Therefore, we deem TACC3 mislocalization from the mitotic spindle as a more robust and uniform marker of Aurora A activity in tissues.

Previous studies in HCT-116 xenografts showed that tumor growth inhibition was maximal in nude mice dosed once a day with a 30 mg/kg oral dose of MLN8054 after 21 days (24). Partial tumor growth inhibition was attained with 3 and 10 mg/kg daily oral dosing of MLN8054. These results are consistent with findings here showing a partial decrease in the percent of spindle localized TACC3 8 h after a 3 and 10 mg/kg oral dose of MLN8054 and a maximal decrease after a 30 mg/kg oral dose. This suggests that the TACC3 mislocalization has potential in predicting outcome in cancer patients treated with MLN8054. Further studies are needed to confirm this hypothesis.

Clinical development of anticancer drugs can be greatly facilitated by implementation of both pharmacokinetic and pharmacodynamic methods that accurately predict clinical outcome. Appropriate measures of the pharmacokinetic/pharmacodynamic relationship in clinical trials provide several advantages, including demonstration of target inhibition, selection of optimal drug dose that maximizes on target efficacy while minimizing off target toxicities, prediction of clinical outcome, and acceleration of the approval process, thereby decreasing the overall cost of drug approval (38). To date, there have been no reports of direct pharmacodynamic markers for measuring Aurora A inhibition. In this report, we show that mislocalization of TACC3 away from mitotic spindles can be used as a robust direct measure of Aurora A activity in tumors. This method should facilitate the clinical advancement of MLN8054 and future Aurora A inhibitors that enter anticancer clinical trials.

Acknowledgments

Received 1/10/2007; revised 3/9/2007; accepted 4/5/2007.

Grant support: Millennium Pharmaceuticals, Inc.

The costs of publication of this article were defrayed in part by the payment of page charges. This article must therefore be hereby marked *advertisement* in accordance with 18 U.S.C. Section 1734 solely to indicate this fact.

We thank the Departments of Medicinal Chemistry, Cancer Pharmacology, and Discovery Technologies at Millennium Pharmaceuticals for the support they provided towards this work; Deborah Wysong for technical assistance; and Drs. Mark Manfredi, Arijit Chakravarty, and Ole Petter Veiby for critical reading of the manuscript.

References

1. Bischoff JR, Anderson L, Zhu Y, et al. A homologue of *Drosophila* aurora kinase is oncogenic and amplified in human colorectal cancers. EMBO J 1998;17:3052–65.
2. Miyoshi Y, Iwao K, Egawa C, Noguchi S. Association of centrosomal kinase STK15/BTAK mRNA expression with chromosomal instability in human breast cancers. Int J Cancer 2001;92:370–3.
3. Sen S, Zhou H, White RA. A putative serine/threonine kinase encoding gene BTAK on chromosome 20q13 is amplified and overexpressed in human breast cancer cell lines. Oncogene 1997;14:2195–200.
4. Sen S, Zhou H, Zhang RD, et al. Amplification/overexpression of a mitotic kinase gene in human bladder cancer. J Natl Cancer Inst 2002;94:1320–9.
5. Tanaka T, Kimura M, Matsunaga K, Fukada D, Mori H, Okano Y. Centrosomal kinase AIK1 is overexpressed in invasive ductal carcinoma of the breast. Cancer Res 1999;59:2041–4.
6. Zhou H, Kuang J, Zhong L, et al. Tumour amplified kinase STK15/BTAK induces centrosome amplification, aneuploidy and transformation. Nat Genet 1998;20:189–93.
7. Goepfert TM, Adigun YE, Zhong L, Gay J, Medina D, Brinkley WR. Centrosome amplification and overexpression of aurora A are early events in rat mammary carcinogenesis. Cancer Res 2002;62:4115–22.
8. Wang X, Zhou YX, Qiao W, et al. Overexpression of aurora kinase A in mouse mammary epithelium induces genetic instability preceding mammary tumor formation. Oncogene 2006;25:7148–58.
9. Zhang D, Hirota T, Marumoto T, et al. Cre-loxP-controlled periodic Aurora-A overexpression induces mitotic abnormalities and hyperplasia in mammary glands of mouse models. Oncogene 2004;23:8720–30.
10. Bischoff JR, Plowman GD. The Aurora/Ipl1p kinase family: regulators of chromosome segregation and cytokinesis. Trends Cell Biol 1999;9:454–9.
11. Carmena M, Earnshaw WC. The cellular geography of aurora kinases. Nat Rev Mol Cell Biol 2003;4:842–54.
12. Giet R, Prigent C. Aurora/Ipl1p-related kinases, a new oncogenic family of mitotic serine-threonine kinases. J Cell Sci 1999;112:3591–601.
13. Goepfert TM, Brinkley BR. The centrosome-associated Aurora/Ipl-like kinase family. Curr Top Dev Biol 2000;49:331–42.
14. Marumoto T, Zhang D, Saya H. Aurora-A: a guardian of poles. Nat Rev Cancer 2005;5:42–50.
15. Nigg EA. Cell division: mitotic kinases as regulators of cell division and its checkpoints. Nat Rev Mol Cell Biol 2001;2:21–32.
16. Barros TP, Kinoshita K, Hyman AA, Raff JW. Aurora A activates D-TACC-Msps complexes exclusively at centrosomes to stabilize centrosomal microtubules. J Cell Biol 2005;170:1039–46.
17. Kinoshita K, Noetzel TL, Pelletier L, et al. Aurora A phosphorylation of TACC3/maskin is required for centrosome-dependent microtubule assembly in mitosis. J Cell Biol 2005;170:1047–55.
18. Peset I, Seiler J, Sardon T, Bejarano LA, Rybina S, Vernos I. Function and regulation of Maskin, a TACC family protein, in microtubule growth during mitosis. J Cell Biol 2005;170:1057–66.
19. Bellanger JM, Gonczy P. TAC-1 and ZYG-9 form a complex that promotes microtubule assembly in *C. elegans* embryos. Curr Biol 2003;13:1488–98.
20. Giet R, McLean D, Descamps S, et al. Drosophila Aurora A kinase is required to localize D-TACC to centrosomes and to regulate astral microtubules. J Cell Biol 2002;156:437–51.
21. Gergely F, Draviam VM, Raff JW. The ch-TOG/XMAP215 protein is essential for spindle pole organization in human somatic cells. Genes Dev 2003;17:336–41.
22. Lee MJ, Gergely F, Jeffers K, Peak-Chew SY, Raff JW. Msps/XMAP215 interacts with the centrosomal protein D-TACC to regulate microtuble behavior. Nat Cell Biol 2001;3:643–9.
23. O'Brien LL, Albee AJ, Liu L, et al. The *Xenopus* TACC homologue, Maskin, functions in mitotic spindle assembly. Mol Biol Cell 2005;16:2836–47.
24. Manfredi MG, Ecsedy JA, Meetze KA, et al. Antitumor activity of MLN8054, an orally active small molecule inhibitor of Aurora A kinase. Proc Natl Acad Sci U S A 2007;104:4106–11.
25. Marumoto T, Honda S, Hara T, et al. Aurora-A kinase maintains the fidelity of early and late mitotic events in HeLa cells. J Biol Chem 2003;278:51786–95.
26. Andrews PD. Aurora kinases: shining lights on the therapeutic horizon? Oncogene 2005;24:5005–15.
27. Keen N, Taylor S. Aurora-kinase inhibitors as anticancer agents. Nat Rev Cancer 2004;4:927–36.
28. Hata T, Furukawa T, Sunamura M, et al. RNA interference targeting aurora kinase a suppresses tumor growth and enhances the taxane chemosensitivity in human pancreatic cancer cells. Cancer Res 2005;65:2899–905.
29. Hirota T, Kunitoku N, Sasayama T, et al. Aurora-A and an interacting activator, the LIM protein Ajuba, are required for mitotic commitment in human cells. Cell 2003;114:585–98.
30. Gygi SP, Han DKM, Gingras AC, Sonenberg N, Aebersold R. Protein analysis by mass spectrometry and sequence database searching: tools for cancer research in the post-genomic era. Electrophoresis 1999;20:310–9.
31. Deutsch E, Jarrousse S, Buet D, et al. Down-regulation of BRCA1 in BCR-ABL-expressing hematopoietic cells. Blood 2003;101:4583–8.
32. Pascreau G, Delcros JG, Cremet JY, Prigent C, Arlot-Bonnemains Y. Phosphorylation of maskin by Aurora-A participates in the control of sequential protein synthesis during *Xenopus laevis* oocyte maturation. J Biol Chem 2005;280:13415–23.
33. Gergely F, Karlsson C, Still I, Cowell J, Kilmartin J, Raff JW. The TACC domain identifies a family of centrosomal proteins that can interact with microtubules. Proc Natl Acad Sci U S A 2000;97:14352–7.
34. Harrington EA, Bebbington D, Moore J, et al. VX-680, a potent and selective small-molecule inhibitor of the Aurora kinases, suppresses tumor growth *in vivo*. Nat Med 2004;10:262–7.
35. Ditchfield C, Johnson VL, Tighe A, et al. Aurora B couples chromosome alignment with anaphase by targeting BubR1, Mad2, and Cenp-E to kinetochores. J Cell Biol 2003;161:267–80.
36. Girdler F, Gascoigne KE, Eyers PA, et al. Validating Aurora B as an anti-cancer drug target. J Cell Sci 2006;119:3664–75.
37. Cheeseman IM, Anderson S, Jwa M, et al. Phospho-regulation of kinetochore-microtubule attachments by the Aurora kinase Ipl1p. Cell 2002;111:163–72.
38. Workman P, Aboagye EO, Chung YL, et al. Minimally invasive pharmacokinetic and pharmacodynamic technologies in hypothesis-testing clinical trials of innovative therapies. J Natl Cancer Inst 2006;98:580–98.

Localization of Human TACC3 to Mitotic Spindles Is Mediated by Phosphorylation on Ser ^{558} by Aurora A: A Novel Pharmacodynamic Method for Measuring Aurora A Activity

Patrick J. LeRoy, John J. Hunter, Kara M. Hoar, et al.

Cancer Res 2007;67:5362-5370.